THE JOURNAL OF PHYSICAL CHEMISTRY B

Letter

Tuning the Electronic Structure of Graphene by an Organic Molecule

Y. H. Lu, W. Chen, Y. P. Feng, and P. M. He

J. Phys. Chem. B, **2009**, 113 (1), 2-5• DOI: 10.1021/jp806905e • Publication Date (Web): 12 December 2008

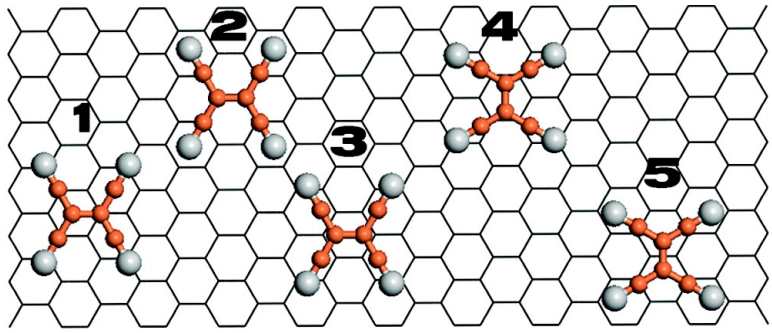

More About This Article

Additional resources and features associated with this article are available within the HTML version:

- Supporting Information
- Access to high resolution figures
- Links to articles and content related to this article
- Copyright permission to reproduce figures and/or text from this article

View the Full Text HTML

THE JOURNAL OF PHYSICAL CHEMISTRY B LETTERS

2009, *113,* 2–5
Published on Web 12/12/2008

Tuning the Electronic Structure of Graphene by an Organic Molecule

Y. H. Lu, W. Chen, and Y. P. Feng*,‡

Department of Physics, National University of Singapore, 2 Science Drive 3, Singapore, 117542

P. M. He*,†

Department of Physics, Zhejiang University, Hangzhou, China, 310027

Received: August 2, 2008; Revised Manuscript Received: September 8, 2008

The electronic structure of an electron-acceptor molecule, tetracyanoethylene (TCNE), on graphene was investigated using the first-principles method based on density functional theory. It was theoretically demonstrated that a p-type graphene can be obtained via charge transfer between an organic molecule and graphene. Both the carrier concentration and band gap at the Dirac point can be controlled by coverage of organic molecules. The spin split and partially filled π^* orbitals of the TCNE anion radical induce spin density in the graphene layer. Surface modification of graphene by organic molecules could be a simple and effective method to control the electronic structure of graphene over a wide range.

Graphene, first isolated by Novoselov,[1] has attracted a lot of attention because of its intriguing physics for fundamental studies and its potential applications for the next-generation electronic devices.[2−6] As a 2D crystal, graphene was found to exhibit high crystal quality,[1,7,8] in which charge carriers can travel thousands of interatomic distances without being scattered.[9−11] In particular, due to its special honeycomb structure, the band structure of graphene exhibits two intersecting bands at two inequivalent K points in the reciprocal space, and its low energy excitations are massless Dirac Fermions near these K points because of the linear (photon-like) energy-momentum dispersion relationship. This results in very high electron mobility in graphene, which can be further improved significantly, even up to $\approx 10^5$ cm^2/V·s. Electron or hole transport in field-effect devices based on graphene can be controlled by an external electric field.[1] Moreover, Park[12] demonstrated theoretically that the chiral massless Dirac Fermions of graphene propagate anisotropically in a periodic potential, which suggests the possibility of building graphene-based electronic circuits from appropriately engineered periodic surface potential patterns, without the need for cutting or etching. Graphene-based devices can be expected to have many advantages over silicon-based devices.

However, precise control of the carrier type and concentration in graphene is not easy, especially for p-type. Up to now, most of the graphene samples were either deposited on a SiO_2 surface or grown on a SiC surface, and these epitaxial graphenes are usually electron doped by the substrate.[13] Alkali metal atoms can be deposited on graphene to selectively control the n-type carrier concentration in the graphene layers. However, distribution of the metal atoms on the graphene surface is usually inhomogeneous, and the resulting charged impurities cause significant reduction of the carrier mobility.[14] The single, open-shell NO_2 molecule is found to be a strong acceptor, whereas its equilibrium gaseous state N_2O_4 acts as a weak dopant and does not result in any significant doping effect.[15] Boron or nitrogen substitutional doping is also not reliable and always induces defects that destroy the promising electronic property of graphene. Thus, it is desirable and crucial to develop new methods to precisely control the carrier type and concentration in graphene for further development of graphene-based nanoelectronics. In addition, pristine graphene is a zero-gap semiconductor, and its Fermi level exactly crosses the Dirac point. For practical application, an energy gap is essential.

Recently, Chen et al.[16] modified the graphene surface using a conjugated organic molecule, F4-TCNQ. They found that electrons transfer from graphene to the adsorbed molecules, resulting in a p-type doped graphene. This opened a door to precisely control the carrier type and concentration of graphene by organic molecules with different electronic properties. It is thus very important to understand the interaction between organic molecules and graphene. However, to our knowledge, there has been hardly any theoretical work on the adsorption of organic molecules on graphene. In this letter, we report results of our first-principles investigation on the adsorption of an interesting molecule, tetracyanoethylene (TCNE), on graphene and the electronic structure of the system. TCNE is an ethene molecule with four hydrogens substituted by cyano, and it is a well-known molecular magnet with a high Curie temperature.[17,18] It is a strong electron acceptor with a large electron affinity that readily forms charge-transfer complexes in which it pulls electrons from neighboring metal atoms or molecules.[19,20] Although the neutral TCNE molecule presents no magnetic properties, its empty antibonding molecular orbitals are spin-polarized, which result in spin-polarized electronic density when they are occupied by electrons.

First-principles calculations were performed using the VASP code.[21−24] The projector augmented wave potentials[25] were used to model electron−ion interactions, while the local spin density approximation (LSDA) was used for the exchange−correlation function. The *k*-space integration was done by summing over the

* To whom correspondence should be addressed.
‡ E-mail: phyfyp@nus.edu.sg.
† E-mail: phypmhe@dial.zju.edu.cn.

10.1021/jp806905e CCC: $40.75

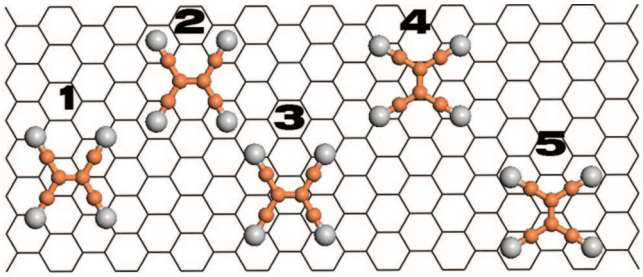

Figure 1. Schematic top view of TCNE on graphene showing five high-symmetry adsorption sites. The black sticks represent the honeycomb structure of graphene, the small orange balls are carbon atoms of TCNE, and the big gray balls are nitrogen atoms of TCNE.

Monkhorst−Pack[26] special points in the 2D Brillouin zone. The tetrahedron method, with a smearing width of 0.1 eV for the Fermi level, was used. The plane wave basis set was restricted by a cutoff energy of 400 eV. The in-plane lattice constant of graphene was set to 2.42 Å, which is the lattice parameter determined from our first-principles calculation within LSDA. In structural optimization, two layers of graphene were used, and the lower layer was kept rigid to model a substrate, while the upper layer, as well as the adsorbed TCNE molecule, was allowed to fully relax. A 20 Å vacuum region was used to ensure that there was negligible interaction between the molecule and the bottom graphene layer in neighboring cells. The forces acting on relaxed atoms were ≤0.02 eV/Å in the optimized structures. Electronic structures of TCNE on a single graphene layer presented below were calculated using the optimized geometries but with the substrate graphene layer removed.

To study the adsorption of an isolated TCNE on graphene, a $4(3)^{1/2} \times 6$ graphene supercell (96 carbon atoms per graphene layer), with one TCNE molecule, was used, and total energy calculations were performed using a $3 \times 3 \times 1$ *k*-point mesh. This ensured a lateral distance between TCNE molecules of at least 10 Å to eliminate interaction between TCNE molecules in neighboring supercells in the dilute limit. The corresponding coverage of TCNE on graphene was 1.04%.

Five high-symmetry adsorption sites of TCNE on graphene are considered in the present study, and they are schematically shown in Figure 1. The central C−C bond of TCNE at sites 1, 2, and 3 is parallel, while that at site 4 and 5 is perpendicular to a C−C bond of graphene. Furthermore, the center of the TCNE molecule is above the hollow site of graphene for binding sites 3 and 4. In contrast, the center of TCNE is over the bridge site of graphene for sites 2 and 5. At site 1, three carbon atoms of the TCNE molecule are over the hollow sites of graphene, while the other three carbons are on top of the carbon atoms of graphene. We first focus our attention on their relative stability. The adsorption energy per TCNE molecule is determined by subtracting the energy of the isolated molecule, E_{TCNE}, and the energy of the substrate, $E_{graphene}$, from the total energy of the TCNE−graphene system $E_{TCNE-graphene}$, that is

$$\Delta E = E_{TCNE-graphene} - E_{graphene} - E_{TCNE} \quad (1)$$

The calculated adsorption energies of TCNE adsorbed at the five sites at the low coverage are given in the first column in Table 1. Although site 4 is the most stable adsorption site, the differences in adsorption energies of various sites are no more than 0.08 eV. In particular, the adsorption energy of TCNE at site 3 is only 0.025 eV higher than that at site 4. Therefore, we predict that the mobility of TCNE on graphene will be high at room temperature. Adsorption of TCNE does not result in any significant structural distortion in the graphene, and the rumpling

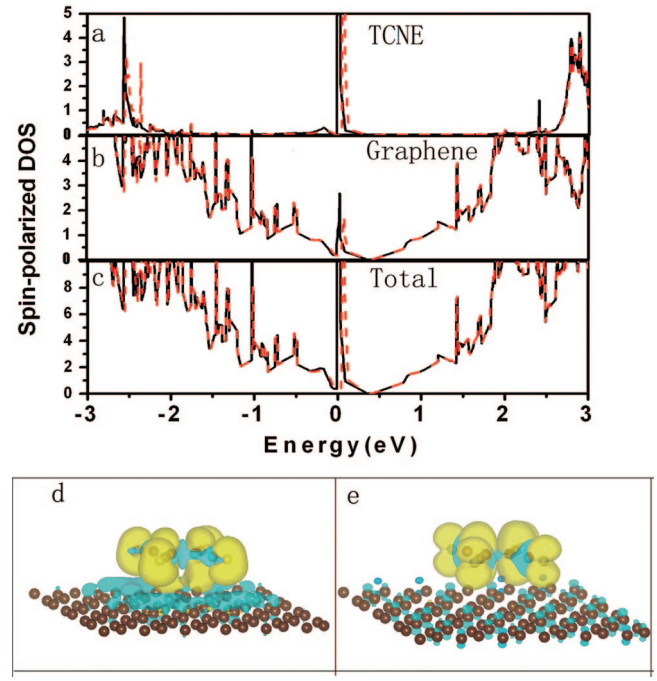

Figure 2. Spin-polarized density of states of TCNE adsorbed on graphene at site 4 (see Figure 1) at low coverage (1 TCNE molecule per supercell containing 96 carbon atoms per layer of graphene) (a) projected on TCNE, (b) projected on graphene, and (c) the total DOS. Black solid (red dashed) lines correspond to spin up (down) states. The Fermi level is set to zero. (d) The 0.003 $Å^{-3}$ differential charge density isosurface. The electron accumulation (depletion) region is indicated by yellow (blue) color. (e) The 0.0002 $Å^{-3}$ spin density isosurface of the TCNE at site 4. The yellow (blue) color represents spin-up (spin-down) electronic density.

of the graphene layer is smaller than 0.1 Å for all adsorption sites considered. For all adsorption sites, the TCNE molecule is found floating above the graphene layer at about 3 Å, and there is no evidence of formation of chemical bonds between the TCNE molecule and the graphene. The interaction between the adsorbed molecule and the substrate is mainly electrostatic in nature, similar to that of TCNE adsorption on a Ag(100) surface.[29] Carbon has a similar electron affinity (1.26 eV[27] on the Bader[28] partition scheme) as Ag (1.30 eV[27]). A charge transfer of ∼0.44 e from graphene to TCNE was found, which results in a strong molecule−substrate interaction and formation of a charge-transfer bond between TCNE and graphene. This can be clearly seen in the differential charge density given in Figure 2d, which is similar to that of TCNE adsorbed on Ag(100).[29] The negatively charged TCNE anions repel each other at high coverage, which will be discussed later.

The differential charge density shown in Figure 2d also reveals that charges transferred from graphene to TCNE are mainly accumulated on nitrogen atoms of cyano and the central sp^2-bonded carbon atom. On the other hand, the charge-depleted area of the graphene plane is delocalized. The band structure around the Dirac point is not significantly affected by the adsorption of TCNE. The calculated total spin-polarized density of states (DOS) of graphene with the adsorbed TCNE (Figure 2c) shows clearly strong acceptor levels at 0.3 eV below the Dirac point. The molecular orbitals of TCNE correspond to flat bands and manifest themselves as peaks in the DOS. The energies of these peaks are nearly independent of the adsorption site. The most interesting feature is the partially occupied molecule orbitals of anion TCNE ($TCNE^-$) around the Fermi level, which is split by the Hund-like exchange interaction (Figure 2a). For a free $TCNE^-$ molecule, the spin-up orbitals are

TABLE 1: Adsorption Energy of TCNE at the Five Sites on Graphene Being Considered (see Figure 1) at Low Coverage (ΔE_1) and High Coverage (ΔE_2)

sites	ΔE_1 (eV)	ΔE_2 (eV)
1	−0.917	−0.534
2	−0.871	−0.651
3	−0.926	−0.528
4	−0.951	−0.616
5	−0.882	−0.529

located at the Fermi level and are partially occupied, while the spin-down orbitals are completely empty. When adsorbed on graphene, the spin-down orbital is 0.07 eV above the Fermi level and remains unoccupied. It is known that the anion $TCNE^-$ is a radical molecule and the partially occupied orbital of $TCNE^-$ is the π^* antibonding molecular orbital.[30] As revealed by the spin density shown in Figure 2e, the spin-up density is mainly localized on the sp^2 carbon and nitrogen atoms, while the spin-down density is localized on the sp carbons of cyano because of the spin delocalization effect and spin polarization effect, which is consist with observation of polarized neutrons experiment.[31] Because of the weak bonding between TCNE and graphene, graphene contributes, through coupling between p_z orbitals of TCNE and graphene, a little to the overall spin (Figure 2e). The graphene band around the Fermi level is also spin-polarized (Figure 2b). At the Fermi level, the density of spin-up electrons dominates over that of spin-down electrons. The large spin-polarization of charge carriers at the Fermi level could be useful for graphene-based spintronic devices, which is expected to have long spin relaxation length.[32]

Next, we consider higher coverage of TCNE molecules on graphene. Here, a $2(3)^{1/2} \times 3$ supercell containing 24 carbon atoms per graphene layer and 1 TCNE was used. The total energy calculations were performed using a $6 \times 6 \times 1$ k-point mesh. As the coverage of TCNE increases, the intermolecular interaction becomes stronger, and the molecule−substrate interaction is weaken. Placing one TCNE molecule per supercell described above results in a TCNE coverage of 4.20% and an intermolecular distance of 2.6 Å. At this small intermolecular separation, the negatively charged TCNE molecules repel each other strongly. The calculated adsorption energies of TCNE at the same five sites shown in Figure 1 are listed in the last column (ΔE_2) in Table 1. They decrease from close to 1 eV in the dilute limit to around 0.6 eV. The strong repulsive intermolecular interaction results in large structural distortion. Figure 3 shows the optimized structure of TCNE adsorbed at site 2 of graphene, which becomes the most stable adsorption site at this high coverage. To lower the repulsive interaction between the negatively charged cyano groups, the TCNE

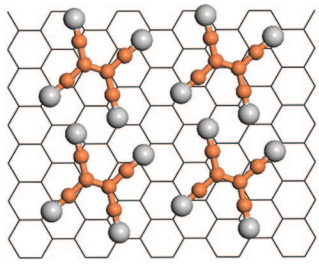

Figure 3. Schematic top view of optimized adsorption structure of TCNE at site 2 (Figure 1) at high coverage (1 TCNE molecule per supercell containing 24 carbon atoms per graphene layer). The black sticks represent the honeycomb structure of graphene, the small orange balls are carbon atoms of TCNE, and the big gray balls are nitrogen atoms of TCNE.

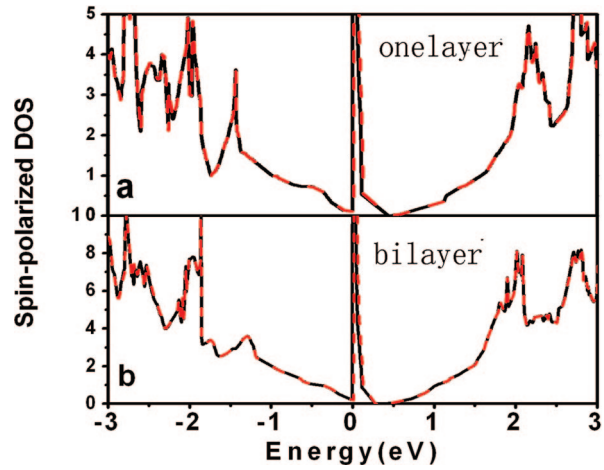

Figure 4. Spin-polarized density of states of (a) TCNE adsorbed on one layer graphene and (b) TCNE adsorbed on bilayer graphene. The black solid (red dashed) lines correspond to spin-up (-down) states. The Fermi levels is set to zero.

molecules rotate by about 30° relative to substrate on all five sites so that the charged cyano groups can avoid facing each other directly. The reduction in intermolecular repulsive interaction results in a lower total energy of the system and site 2 as a more stable adsorption site, compared to site 4, which is the most stable adsorption site in the dilute limit. The rotation of the molecule reduces the intermolecule interaction but raises the molecule−substrate interaction. At site 4, the increase in the molecule−substrate interaction is more than that at site 2, although the TCNE molecules rotate by roughly the same angle in both cases.

Also due to the strong intermolecular repulsive interaction, the amount of charge transfer from graphene to TCNE decreases. Compared to the charge transfer of ∼0.44 e per TCNE molecule from graphene to TCNE in the dilute limit, only 0.2 e of charge is transferred from graphene to each TCNE molecule at this high coverage. However, due to more TCNE molecules per unit surface area, the overall charge transfer from graphene to the TCNE molecules is more efficient. Considering that the TCNE coverage in the high-coverage case considered here is four times that in the dilute limit, the charge transfer per unit area of graphene actually increases by 80% compared to that in the dilute limit. Due to the charge depletion in graphene, the work function of graphene increases to 4.91 eV at the low TCNE coverage and 5.09 eV at the high coverage, from 4.41 eV for clean graphene. Therefore, the high coverage of TCNE leads to more efficient p-doping of graphene. At the coverage of 4.20%, the Dirac point of graphene shifts from 0.3 to 0.5 eV above the Fermi level (Figure 4a). However, this may not be a general behavior for all organic molecules. If the interaction between molecules is too strong, the amount of charge transfer may be insufficient to produce efficient p-doping. It is thus important to choose the right electron-acceptor molecule in order to achieve p-doped graphene. The spin polarization, which is mainly determined by the amount of charge transfer from graphene to TCNE, was found to be reduced when the coverage of TCNE increased. Figure 4a shows the spin-polarized DOS at the high coverage. Compared to that in Figure 2c, the splitting of the partially occupied molecular orbitals around the Fermi level is significantly reduced, and the spin-up and spin-down energy levels become almost degenerate because of less electrons gained by each TCNE molecule. The magnetic momentum of the system becomes 0.05 μB per TCNE, and no significant spin density is observed on graphene. The reduced charge transfer from graphene to each TCNE molecule also weakens the charge-transfer

bond between TCNE and graphene, which is reflected by the smaller adsorption energy (Table 1).

It has been demonstrated that an energy gap opens at the Dirac point if two graphene layers in a bilayer system are inequivalent.[33,34] For bilayer graphene, the band structure at the K point consists of a pair of π and π^* bands which are separated by a gap and another degenerate pair of π and π^* bands at which the Fermi level crosses. This degeneracy is removed when the equivalence of the two graphene layers is broken by charge accumulation in one of the graphene layer or by an external electrostatic potential. In the TCNE/graphene system, the charge depletion in the graphene layer adsorbed with TCNE causes the inequivalence between the two graphene layers and the gap opening at the K point. The calculated total DOS of the TCNE−bilayer-graphene at the high coverage (one TCNE molecule per $2(3)^{1/2} \times 3$ supercell) is shown in Figure 4b. Due to charge depletion in the graphene layer adsorbed with TCNE, the potential equivalence between two layers is broken, and an energy gap of ~0.23 eV is open at the Dirac point above the Fermi level. The size of the gap was found to increase with charge depletion in graphene. Since the amount of charge transfer from graphene to TCNE varies with TCNE coverage, the energy gap of graphene can be tuned by the coverage of TCNE on the bilayer graphene. For example, at the low coverage of one TCNE molecule per $4(3)^{1/2} \times 6$ supercell, the gap is reduced to 0.04 eV. Graphene can now be easily grown on SiC. It can be expected that when TCNE is adsorbed on bilayer graphene grown on a SiC substrate, the charge difference or Coulomb potential difference between the two graphene layers will be larger due to excess charge in the graphene layer next to SiC gained from the substrate.[33] The width of the energy gap would be larger than that of the free-standing TCNE−bilayer-graphene. By selecting the proper molecule and substrate, the width of the band gap of graphene may be tuned over a wider range. TCNE molecules are more advantageous compared to alkali atoms because the intermolecular repulsive interaction leads to uniform distribution of the molecules at increasing coverage.[14]

The P−N junction is a basic unit in integrated circuits, and it is desirerable to fabricate P−N junctions on a graphene layer for graphene-based electronic devices. An organic molecule may be useful for achieving this goal. For example, using graphene grown on a SiC substrate, p-type domains can be created through self-assembly of acceptor molecules[35] such as TCNE in selected areas on graphene, while the undoped regions are naturally n-type domain.[13] Modification of graphene with patterned two-dimensional supermolecules of acceptor and donor types[36] could be another way to obtain an array of P−N junctions on graphene. Furthermore, a periodic potential due to patterned organic molecules on the graphene surface may also lead to other interesting and potentially useful behaviors of charge carriers. For example, the transport of charge carriers through such a graphene superlattice can be highly anisotropic, and in extreme cases, the group velocities can be reduced to zero in one direction but unchanged in another.[12] An important suggestion of the present study is the possibility of building graphene electronic circuits without the need for cutting or etching the graphene.

In summary, we investigated the detailed electronic structure of TCNE on graphene. Our results demonstrate that p-type graphene can be obtained by modifying the graphene with electron-acceptor molecules. The stable adsorption site of TCNE on graphene varies with coverage due to competition of intermolecular repulsive electrostatic interaction and the molecule−substrate interaction. The Fermi level shifts downward relative to the Dirac point when the TCNE coverage increases, providing a simple and nondestructive way of controlling the hole concentration in graphene. The split and partially filled π^* orbitals of the TCNE anion radical induce a small but significant spin density in the graphene layer at low coverage, and states at the Fermi level are composed mainly of the spin-up states, which is potentially useful for spintronics applications. When TCNE is adsorbed on one side of a bilayer graphene, a band gap as large as 0.23 eV opens at the Dirac point, which can be further tuned by TCNE coverage. Our work demonstrates that the electronic structure of graphene can be controlled over a wider range by organic molecules, and it is thus possible to build graphene-based electronic devices by modifying the graphene with patterned organic molecules, without the need for cutting or etching graphene.

Acknowledgment. The authors wish to thank the Center for Computational Science & Engineering of National University of Singapore.

References and Notes

(1) Novoselov, K. S.; et al. *Science* **2004**, *306*, 666.
(2) Schedin, F.; et al. *Nat. Mater.* **2007**, *6*, 652.
(3) Berger, C.; et al. *Science* **2006**, *312*, 1191.
(4) Han, M. Y.; et al. *Phys. Rev. Lett.* **2007**, *98*, 206805.
(5) Rycerz, A.; Tworzydlo, J.; Beenakker, C. W. J. *Nat. Phys.* **2007**, *3*, 172.
(6) Huard, B.; et al. *Phys. Rev. Lett.* **2007**, *98*, 236803.
(7) Stankovich, S.; et al. *Nature* **2006**, *442*, 282.
(8) Meyer, J. C. et al. *Nature*In press; doi:10.1038/nature05545.
(9) Novoselov, K. S.; et al. *Proc. Natl. Acad. Sci. U.S.A.* **2005**, *102*, 10451.
(10) Novoselov, K. S.; et al. *Nature* **2005**, *438*, 197.
(11) Zhang, Y.; Tan, J. W.; Stormer, H. L.; Kim, P. *Nature* **2005**, *438*, 201.
(12) Park, C. H.; Yang, L.; Son, Y. W.; Cohen, M. L.; Louie, S. G. *Nat. Phys.* **2008**, *4*, 213.
(13) Zhou, S. Y.; Gweon, G.-H.; Fedorov, A. V.; First, P. N.; De Heer, W. A.; Lee, D.-H.; Guinea, F.; Castro Neto, A. H.; Lanzara, A. *Nat. Mater.* **2007**, *6*, 770.
(14) Chen, J. H.; Jang, C.; Adam, S.; Fuhrer, M. S.; Williams, E. D.; Ishigami, M. *Nat. Phys.* **2008**, *4*, 377.
(15) Wehling, T. O.; Novoselov, K. S.; Morozov, S. V.; Vdovin, E. E.; Katsnelson, M. I.; Geim, A. K.; Lichtenstein, A. I. *Nano Lett.* **2008**, *8*, 173.
(16) Chen, W.; Chen, S.; Qi, D. C.; Gao, X. Y.; Wee, A. T. S. *J. Am. Chem. Soc.* **2007**, *129*, 10418.
(17) Manriquez, J. M.; Yee, G. T.; McLean, R. S.; Epstein, A. J.; Miller, J. S. *Science* **1991**, *252*, 1415.
(18) Jain, R.; Kabir, K; Gilroy, J. B.; Mitchell, K. A. R.; Wong, K.; Hicks, R. G. *Nature* **2007**, *445*, 291.
(19) Foster, R. *Organic Charge-Transfer Complexes*; Academic Press: New York, 1969.
(20) Masnovi, J. M.; Kochi, J. K. *J. Am. Chem. Soc.* **1985**, *107*, 6781.
(21) Kresse, G.; Hafner, J. *Phys. Rev. B* **1993**, *47*, 558.
(22) Kresse G. Ph. D. Thesis, Technische University Wien, Austria, 1993.
(23) Kresse, G.; Furthmüller, J. *Phys. Rev. B* **1996**, *54*, 11169.
(24) Kresse, G.; Furthmüller, J. *Comput. Mater. Sci.* **1996**, *6*, 15.
(25) Kresse, G.; Joubert, D. *Phys. Rev. B* **1999**, *59*, 1758.
(26) Monkhorst, H. J.; Pack, J. D. *Phys. Rev. B* **1976**, *13*, 5188.
(27) Lide, D. R. *CRC Handbook of Chemistry and Physics*, 85th ed.; CRC Press: Boca Raton, FL, 2004.
(28) Henkelman, G.; Arnaldsson, A. *J. Mater. Sci.* **2006**, *36*, 254.
(29) Wegner, D.; Yamachika, R.; Wang, Y.; Brar, V. W.; Bartlett, B. M.; Long, J. R.; Crommie, M. F. *Nano Lett.* **2008**, *8*, 131.
(30) Ressouche, E.; Schweizer, J. *Monatsh. Chem.* **2003**, *134*, 235.
(31) Zheludev, A.; Grand, A.; Ressouche, E.; Schweizer, J.; Morin, B. G.; Epstein, A. J.; Dixon, D. A.; Miller, J. S. *J. Am. Chem. Soc.* **1994**, *116*, 7243.
(32) Tombros, N.; Jozsa, C.; Popinciuc, M.; Jonkman, H. T.; Wees, B. J. *Nature* **2007**, *448*, 571.
(33) Ohta, T.; Bostwick, A.; Seyller, T.; Horn, K.; Rotenberg, E. *Science* **2006**, *313*, 951.
(34) Jeroen, B. O.; Hubert, B. H.; Liu, X. L.; Alberto, M; Lieven, M. K. V. *Nat. Mater.* **2007**, *7*, 151.
(35) Stawasz, M. E.; Sampson, D. L.; Parkinson, B. A. *Langmuir* **2000**, *16*, 2326.
(36) Feyter, S. D.; Schryver, F. D. *Chem. Soc. Rev.* **2003**, *32*, 139.

JP806905E